# Virtual Experiments on Complex Materials

Gary W Delaney*, Shio Inagaki, T. Di Matteo and Tomaso Aste
*Department of Applied Mathematics,*
*The Australian National University, Australia*

We investigate complex materials by performing "Virtual Experiments" starting from three-dimensional images of grain packs obtained by X-ray CT imaging [1]. We apply this technique to granular materials by reconstructing a numerical samples of ideal spherical beads with desired (and tunable) properties. The resulting "virtual packing" has a structure that is almost identical to the experimental one. However, from such a digital duplicate we can calculate several static and dynamical properties (e.g. the force network, avalanche precursors, stress paths, stability, fragility, etc.) which are otherwise not directly accessible from experiments. Our simulation code handles three-dimensional spherical grains and it takes into account repulsive elastic normal forces, frictional tangential forces, viscous damping and gravity. The system can be both simulated within a vessel or with periodic boundary conditions.

## I. INTRODUCTION

We are surrounded in our everyday lives by granular matter, with a great many important natural systems, such as sand and soil, being composed of granular packings [2]. They are also of great industrial importance, with granular packings playing an important role in a number of our industries, including construction, mining and pharmaceuticals [3]. These packings can be composed of grains of an arbitrary shape [4], though spherical or near spherical grains are common and are widely chosen in experimental and numerical investigations due to the relative ease with which grain interactions can be characterised. Indeed, sphere packings have long been studied and are widely considered to be systems that can yield important insights into the complex behavior of granular matter [5, 6]. Recently X-ray computed tomography has been used with great success to image and analyze large packings composed of over 100,000 spheres (see Figure 1) [1, 7, 8]. This has yielded new insights into the internal structure and properties of large sphere packings [9].

Here we will utilise the sphere coordinates obtained from the tomographic data as an input into a Discrete Element Method (DEM) simulation. The Discrete Element Method is a numerical method for the simulation of the motion of collections of individual particles / grains [10]. The central requirement for its application is that the system under consideration is composed of discrete particles / grains. DEM has been used extremely successfully in many

* gary.delaney@anu.edu.au

Complex Systems II, edited by Derek Abbott, Tomaso Aste, Murray Batchelor, Robert Dewar,
Tiziana Di Matteo, Tony Guttmann, Proc. of SPIE Vol. 6802, 68020G, (2008)
0277-786X/08/$18 · doi: 10.1117/12.759412

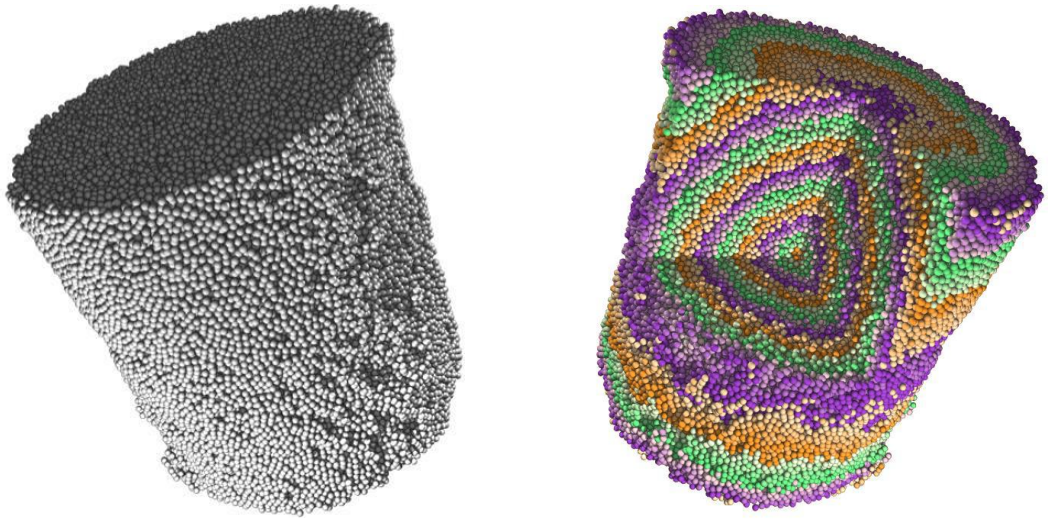

**FIG. 1:** (Left) Tomographic reconstruction of a packing of 150,000 spheres in a cylindrical container. (Right) A portion of the sample is removed and the topological distances from a given central sphere are highlighted in color [1].

areas of science, and has been applied to the simulation of liquids, bulk materials, powders and a large variety of granular matter including sand, cereals and soil [2, 11–13].

Our motivation in applying the DEM technique here is two-fold. Firstly, we wish to better characterise our experimental packing by removing the uncertainty in the exact locations of the sphere centers ($< 0.1\%$) and also the uncertainty in the exact diameters of the spheres caused by sample spheres having a polydispersity of approximately 2%. This allows us to produce a simulated ideal mono-disperse sphere packing that almost exactly matches the original experimental packing. To achieve this, we perform a DEM simulation using mono-disperse spheres positioned at the experimentally obtained sphere centers and allow the system to relax to a stable configuration. With this packing we can achieve our second goal of examining the static and dynamical properties of the system (e.g. the force network, avalanche precursors, stress paths, stability, fragility, etc.), which cannot easily be determined from the raw tomographic data. In this paper, we will outline our simulation technique and demonstrate how in applying this technique we are able to produce a simulated packing that is almost identical to our original experimental one, but that is easily characterisable, with the uncertainties in the tomographic data no longer present.

## II. SIMULATION

In our simulation we consider a mono-disperse packing of elastofrictional spheres. Hertz showed that two identical spherical grains of diameter $d$ interact with a normal repulsive force $F_n$ which is proportional to the overlap $\xi_n$ of two interacting spheres with

$$F_n = k_n \xi_n^{3/2} \tag{1}$$

with $\xi_n = d - |\vec{r}_i - \vec{r}_j|$, where $d$ is the sphere-diameter and $\vec{r}_i$ and $\vec{r}_j$ are the positions of the grain centers [14, 15]. This force only acts when grains overlap, with $F_n = 0$ for $\xi_n < 0$. We consider the tangential force $F_t$ on our spherical grains under oblique loading using

$$F_t = -\min(|k_t \xi_n^{1/2} \xi_t|, |\mu F_n|) \cdot \mathrm{sign}(v_t) \tag{2}$$

where $\xi_t$ is the displacement in the tangential direction that has taken place since the time $t_o$ when the two spheres first get in contact, $v_t$ is the relative shear velocity and $\mu$ is the kinematic friction coefficient between the spheres [10]. We also include a normal viscoelastic dissipation $F_n = -\gamma_n \xi_n^{1/2} \dot{\xi}_n$ (with $\dot{\xi}_n$ the normal velocity) and a viscous friction force $F_t = -\gamma_t v_t$ [16].

In the simulation presented in this paper we normalise the diameter of the spheres ($d = 1$), the mass of the spheres ($m = 1$) and the acceleration due to gravity ($g = 1$). We fix the kinematic friction coefficient $\mu = 0.4$ and consider stiff grains with $k_n \sim 10^5$, corresponding to spheres with a Young's modulus $E \sim 10MPa$. The ratio of $k_t/k_n$ is set to 0.4. In future work, we will investigate the influence of varying these parameters, in particular considering stiffer grains with larger values of $E = 100MPa$ and $E = 1GPa$.

## III. DEM RELAXATION OF EXPERIMENTAL SAMPLES

We consider an experiment with mono-sized acrylic beads packed in a cylindrical container with an inner diameter of 55 mm and filled to a height of ∼75 mm. The packing is composed of 36461 spheres packed at a density $\rho = 0.64 \pm 0.005$. The experimental packing was obtained by a combined action of gentle tapping and compression from above. To reduce the effect from the boundary, the container was roughened by randomly gluing spheres to the internal surfaces. The location of the sphere centers was then obtained from a tomographic reconstruction and these were used as the input for our simulation [1, 8]. The spheres located at the sides and the bottom of the sample (within four diameters of the boundaries) were fixed in position. The top of the system is left open to allow for the possibility of small expansions of the system during the relaxation process.

The DEM simulation is then performed on the unfixed spheres in the central region of the sample, with the boundaries provided by the outer fixed spheres. Figure 2 shows the variation in the average height of the grains as the simulation proceeds. There is initially

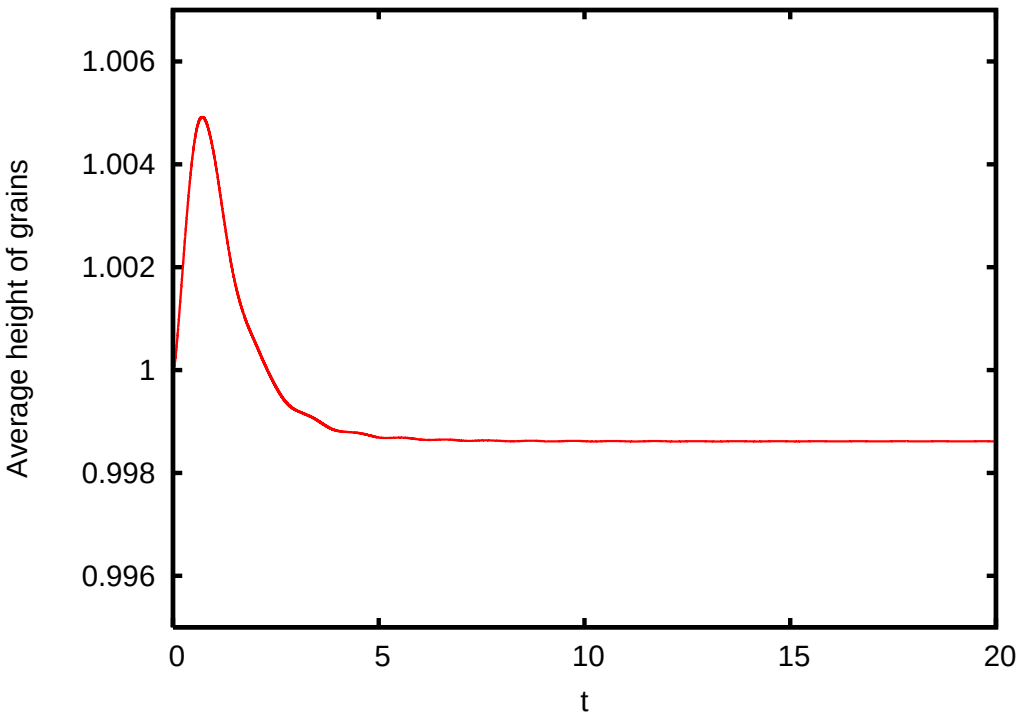


**FIG. 2:** The variation of the average height of the grain centers during the simulation (normalised to 1 for the initial average height).

a small expansion of the system, with the height increasing by $\sim 0.5\%$. The viscoelastic dissipation and viscous friction forces described in the previous section remove energy from the system until the spheres have all settled down to a stationary state. The final average height of the grains is within 0.2% of the initial average height and the average displacement of the centers of the spheres during the relaxation process is less than 4% of the sphere diameters.

## IV. NUMBER OF NEIGHBORS

The average number of neighbors in contact with any given sphere in the packing is a simple and important measure of the system's topological structure. Figure 3 shows the comparison between the behavior of the average number of sphere centers $n_t(r)$ within a radial distance $r$ obtained from both our DEM simulation and the original tomographic data. In the original data it is clear that the determination of the average number of neighbors in contact is extremely difficult as the data shows a slow smooth increase in the number of

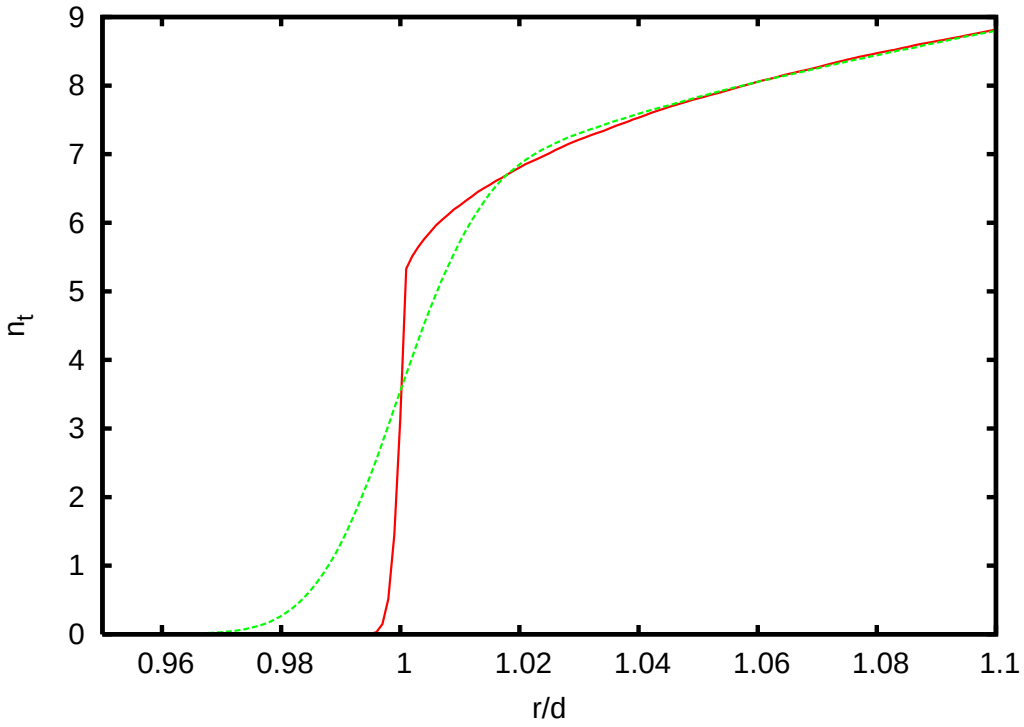


**FIG. 3:** Average number of sphere centers within a radial distance $r$ for the original experiment (green dotted-line) and the virtual experiment (red solid-line).

neighbors over a range of $r = 0.97d \rightarrow 1.02d$. Conversely, our virtual experiment shows a much sharper increase in the number of neighbors, with the discontinuity at $r \simeq d$ giving a good estimate of the actual average number of contacts which can be estimated at $n_c \simeq 5.3$.

## V. RADIAL DISTRIBUTION FUNCTION

The radial distribution function $g(r)$ is associated to the probability of finding the center of a sphere in a given position at distance $r$ from a reference sphere. The radial distribution function is calculated by counting the number of sphere centers within a radial distance $r$ from a given sphere center $(n_t(r))$ and using

$$n_t(r_1) - n_t(r_o) = \int_{r_o}^{r_1} g(r) 4\pi r^2 \, dr. \tag{3}$$

This function is widely used in the geometrical characterization of granular packings. Figure 4 shows the radial distribution function $\tilde{g}(r)$ (which has been normalised such that $\tilde{g}(r) \rightarrow 1$

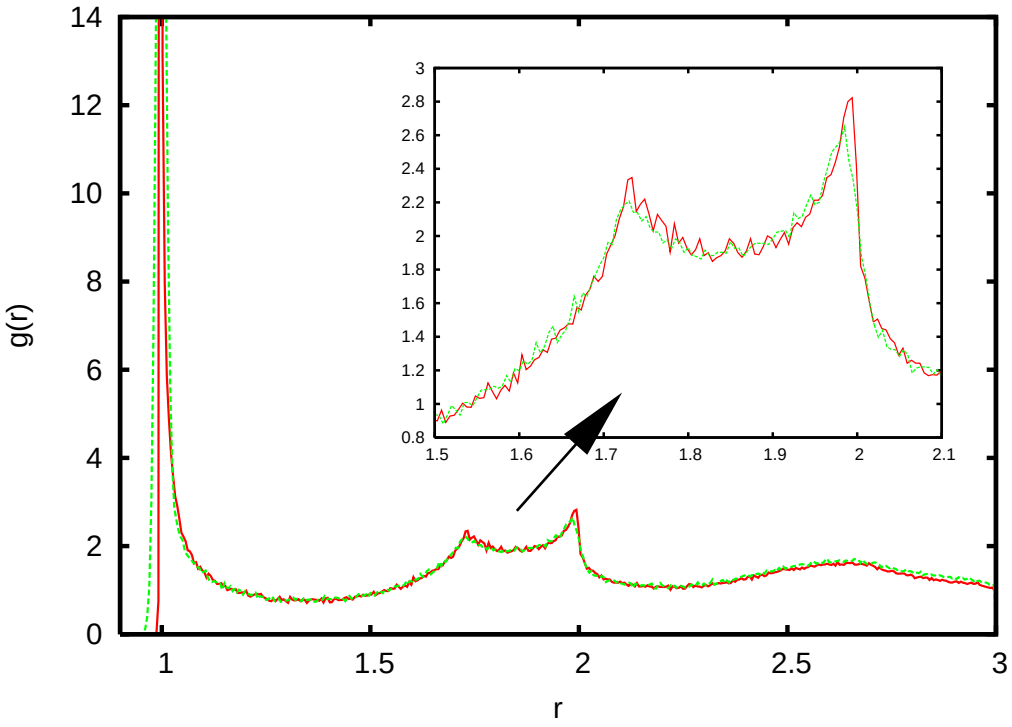


**FIG. 4:** Average number of sphere centers within a radial distance $r$ for the original experiment (green dotted-line) and the virtual experiment (red solid-line).

for $r \to \infty$) for both our DEM simulation and the original tomographically obtained data. Both sets of data show a strong peak at $r = d$, with this peak being much sharper in the DEM simulation. We also observe two peaks at $r = \sqrt{3}d$ and $r \simeq 2d$, which are again sharper in the DEM simulation.

## VI. CONCLUSIONS AND OUTLOOK

In this paper we have shown how DEM can be used to perform a virtual experiment, using as an input tomographic sphere packing data. We have applied this technique to a sample case-study, demonstrating that such a technique is useful in identifying structural properties such as the number of grains in contact or the peaks in the radial distribution function. These results show that the technique is reliable and the resulting packing after DEM relaxation is almost identical to the experimental one, but with the uncertainty in grain diameter and grain location removed. This technique can now be applied to study other properties of the system that cannot be obtained experimentally. These include characterisation of the

force network and stress paths within the packing and their behavior when the system is put under different loadings. In future work, we will also investigate the factors contributing to the stability of the packing and seek to identify the presence of avalanche precursors within the system.

## VII. ACKNOWLEDGEMENTS

Many thanks to T.J. Senden and M. Saadatfar for the tomographic data. This work was partially supported by the ARC discovery Project No. DP0450292 and Australian Partnership for Advanced Computing National Facility (APAC).

[1] T. Aste. Variations around disordered close packing. *J. Phys. Condensed Matter*, 17(24):S2361–S2390, June 2005.
[2] L. P. Kadanoff. Built upon sand: Theoretical ideas inspired by granular flows. *Rev. Mod. Phys.*, 71(1):435–444, 1999.
[3] P. G. de Gennes. Granular matter: a tentative view. *Rev. Mod. Phys.*, 71(2):S374–S382, 1999.
[4] G. Delaney, D. Weaire, S. Hutzler, and S. Murphy. Random packing of elliptical disks. *Phil. Mag. Lett.*, 85(2):89–96, 2005.
[5] J. D. Bernal and J. Mason. Co-ordination of randomly packed spheres. *Nature*, 188(4754):910–911, 1960.
[6] S. Hutzler, G. Delaney, D. Weaire, and F. MacLeod. Rocking newton's cradle. *Am. J. Phys.*, 72(12):1508–1516, 2004.
[7] T. Aste, M. Saadatfar, A. Sakellariou, and T. J. Senden. Investigating the geometrical structure of disordered sphere packings. *Physica A*, 339(1-2):16–23, August 2004.
[8] T. Aste, M. Saadatfar, and T. J. Senden. Geometrical structure of disordered sphere packings. *Phys. Rev. E*, 71(6):061302, June 2005.
[9] T. Aste. Volume fluctuations and geometrical constraints in granular packs. *Phys. Rev. Lett.*, 96(1):018002, January 2006.
[10] P. A. Cundall and O. D. L. Strack. Discrete numerical-model for granular assemblies. *Geotechnique*, 29(1):47–65, 1979.
[11] T Aste and D Weaire. *The Pursuit of Perfect Packing.* Bristol and Philadelphia: IOP Publishing Ltd, 2000.
[12] H. M. Jaeger, S. R. Nagel, and R. P. Behringer. Granular solids, liquids, and gases. *Rev. Mod. Phys.*, 68(4):1259–1273, 1996.
[13] Liu A J and Nagel S R. *Jamming and Rheology.* London, New York: Taylor and Francis, 2001.
[14] L.D. Landau and E.M. Lifshitz. *Theory of Elasticity.* Pergamon, New York, 1970.
[15] H. A. Makse, N. Gland, D. L. Johnson, and L. Schwartz. Granular packings: Nonlinear elasticity, sound propagation, and collective relaxation dynamics. *Phys. Rev. E*, 70(6):061302, December 2004.

[16] J. Schafer, S. Dippel, and D. E. Wolf. Force schemes in simulations of granular materials. *Journal de Physique I*, 6(1):5–20, January 1996.